Designer antisense circRNA$_{GFP}$ reduces GFP protein abundance in transgenic Arabidopsis protoplasts in a sequence-specific manner, independent of RNAi pathways

[1]Hossain M, [2]Pfafenrot C, [1]Imani J, [1]Šečić E, [3]Sede A, [1]Galli M, [3]Heinlein M, [2]Bindereif A, [1]Ladera-Carmona M, [1]Kogel KH.

[1]Institute of Phytopathology, Centre for BioSystems, Land Use and Nutrition, Justus Liebig University, Heinrich-Buff-Ring 26, D-35392, Giessen, Germany

[2]Institute of Biochemistry, Heinrich-Buff-Ring 17, Justus Liebig University, D-35392 Giessen, Germany

[3]Institut de biologie moléculaire des plantes, CNRS, Université de Strasbourg, 12 rue du Général Zimmer, 67084 Strasbourg, France

Word count:

Keywords: antisense RNA, Arabidopsis, circular RNA, gene silencing, protoplast transfection, small RNA

[#] Corresponding author:

karl-heinz.kogel@agrar.uni-giessen.de (ORCID no.: 0000-0003-1226-003X)

All E-mail addresses:

Moammar.Hossain@agrar.uni-giessen.de (ORCID no.: 0009-0006-1528-4167)
Christina.Pfafenrot@gmx.de (ORCID no.: 0009-0009-1846-3613)
jafargholi.imani@agrar.uni-giessen.de (ORCID no.: 0000-0001-8265-1656)
Ena.Secic@agrar.uni-giessen.de (ORCID no.: 0000-0002-6469-4895
ana.sede@ibmp-cnrs.unistra.fr (ORCID no.: 0000-0002-7868-0638)
Matteo.Galli@transmit.de (ORCID no.:) 0000-0003-4514-9434

manfred.heinlein@ibmp-cnrs.unistra.fr (ORCID no.: 0000-0001-7322-1654)
albrecht.bindereif@chemie.bio.uni-giessen.de (ORCID no.: 0000-0002-7730-7380)
Maria.Ladera-Carmona@agrar.uni-giessen.de (ORCID no.: 0000-0003-2167-3135)

Abstract:

Circular RNAs (circRNAs) are single-stranded molecules that have attracted increasing attention in recent years due to their covalently closed structure and their diverse functional roles in mammalian cells, where they are involved in the regulation of gene expression and protein function. Increasing evidence suggests that circRNAs have similar functions in plants, where they play a role in plant development, resistance to biotic stress, and abiotic stress tolerance. Here, we investigated the agronomically relevant question of whether synthetic designer circRNAs can be used to modulate in a sequence-specific manner gene expression in plants. We show that treatment of *GFP*-expressing Arabidopsis protoplasts with designer 50 nt GFP antisense circRNA ($circRNA_{GFP}$) reduces the cellular accumulation of the reporter protein in a sequence-specific and dose-dependent manner. This inhibitory activity of $circRNA_{GFP}$ was not abolished in various Arabidopsis *ago* and *dcl* mutants with defective RNAi pathways. Moreover, and in contrast to other types of RNA such as double-stranded (ds)RNA, circRNAs did not induce a PTI response in plant leaves. We discuss the possibility that circRNA may be applied to regulate endogenous plant genes and thus may have future potential as a novel bioherbicide.

Introduction

Agricultural production is affected by a variety of biotic and abiotic stress factors, which will increase due to higher temperatures and extreme weather conditions as a result of climate change (IPPC Secretariat, 2021; Pareek et al., 2020). Further improvement or even maintenance of global yield levels will depend to a large extent on new scientific solutions and their rapid introduction into agronomic practice (Lamichhane et al., 2016; Van Dijk et al., 2021). Farmers around the world are still looking for effective measures, including the use of pesticides or nature-based substances and beneficial microbes as biological control agents (Köhl et al., 2019). While there is a broad consensus in the scientific community and clear legal requirements in most countries request that synthetic pesticides, including herbicides, should be used as little as possible (Deguine et al., 2021), alternative crop protection measures are being developed, but their efficacy in intensive production systems has rarely been demonstrated and their

dependence on environmental factors is only poorly investigated (Kremer et al., 2023; Perez-Alvarez et al., 2019).

Recent findings raise hopes that treatments with ribonucleic acids (RNAs) have interesting potential to reduce diseases in plants and animals, including humans (Cai et al., 2018; Kulkarni et al., 2021; Liu et al., 2020; Winkle et al., 2021). RNA is the essential component of the genetic template of the first life forms and has evolved in higher life forms to become a central molecule involved in the storage, transmission, and modification of genetic information. It is also involved in communication between interacting organisms, such as animal and plant hosts and their pathogens, a phenomenon known as cross-kingdom RNA interference (ckRNAi; Buck et al., 2014; LaMonte et al., 2012; Shahid et al., 2018; Weiberg et al., 2013; Zhang et al., 2016). In higher organisms, RNA exists predominantly in the linear form as protein-coding mRNA and non-coding forms, such as ribosomal (r)RNAs, long non-coding RNA (lncRNA), transfer (t)RNAs and different types of small (s)RNAs of 21 to 24 nucleotides (nt). For the latter, their high significance for regulatory processes such as maintenance of genome stability and regulation of gene activity had only been found in 1998, when their function in RNA interference (RNAi) was discovered (Baulcombe et al., 2004; Fire et al., 1998; Ghildiyal and Zamore, 2009).

Consistent with their role in natural communication between plant hosts and microbial pathogens or parasitic weeds, artificial RNAs, such as sRNA duplexes or double-stranded (ds)RNAs containing up to several hundred nucleotides, can protect plants from biotic stress. These include strategies that involve the production of RNA in transgenic plants (host-induced gene silencing, HIGS) and spray application of exogenous RNA (spray-induced gene silencing, SIGS) (for review see Cai et al., 2018; Fletcher et al., 2020; Koch and Wassenegger, 2021; Liu et al., 2020; Taning et al., 2019). While HIGS strategies are highly effective and ecologically superior from a scientific perspective, they are politically undesirable at least in most European countries. In fact, SIGS applications may have some advantages over HIGS approaches because, at least in theory, the RNA agent can be adapted very quickly to combat very different biotic stresses. However, while SIGS applications show promising results in some examples (Koch et al., 2016; Sarkar et al., 2021; Walker et al., 2023; Wang et al., 2016; Werner et al., 2021), the type of RNAs used for the application, currently dsRNA and sRNA, are susceptible to degradation, especially if they are not protected by chemical formulations (Chu et al., 2023; Mitter et al., 2017). Moreover, the risk of genetic cross-resistance to the active compounds in the target microbe, pest or weed is a realistic scenario in which the RNAi components and uptake mechanisms are susceptible to counter-selection (Khajuria et al., 2018; Mishra et al.,

2021; Šečić et al., 2021; Wytinck et al. 2020). Therefore, it is a reasonable scientific goal to search for new RNA-based active substances with as many different modes of action as possible.

In addition to its main use as a biological control agent against microbial pathogens and animal pests, there is growing interest in exploring the potential use of RNA for weed control (Mai et al., 2021; Zabala-Pardo et al., 2022). However, there are challenges for using SIGS as a practical tool for weed management. Most critically, and apart from its susceptibility to degradation, several authors reported that dsRNA and sRNA can hardly penetrate into plant leaves at levels that induce silencing of plant genes (Bennett et al., 2020; Dalakouras et al., 2016; Liu et al., 2021). To overcome the challenges, it is necessary *i.* to develop efficient RNA formulations to increase uptake and *ii.* to explore activities of RNA molecules other than dsRNA and sRNA as alternatives.

In the search for new types of RNAs with different modes of action, we investigated the possibility of using circular RNA (circRNA) for plant protection. Unlike linear RNA (linRNA) molecules, circRNAs form a covalently closed loop, which confers resistance to exonucleases, making them more stable and resistant to degradation (Nielsen et al., 2022). This circularization can be achieved through a process known as back-splicing, in which a downstream splice donor site joins with an upstream splice acceptor site, resulting in the formation of a closed loop. circRNAs can arise from exons (exonic circRNA), introns (intronic circRNA), and intergenic regions (Jeck and Sharpless, 2014; Zhang et al., 2013). Initially considered as splicing errors or byproducts of mRNA processing, circRNAs have emerged as a new and complex class of RNA molecules with a wide range of biological functions (Cocquerelle et al., 1993; Hansen et al., 2013; Hsu and Coca-Prados, 1979; Memczak et al., 2013). Knowledge about circRNAs has been generated mainly in animal systems, where they are involved in regulating gene expression at multiple levels, including their function as microRNA (miRNA) sponges (binding to miRNAs and repressing their function), as protein scaffolds, or in sequestration and translocation of proteins, facilitation of interactions between proteins and translation into proteins (Guo et al., 2014; Hansen et al., 2013; Jeck et al. 2013; Jeck and Sharpless, 2014; Nielsen et al., 2022). Moreover, circRNAs are known to modulate various physiological processes such as cell differentiation, development, and cellular immune responses, and play a role in numerous diseases, including cancer and neurological disorders, with their therapeutic potential widely recognized (He et al., 2021). circRNAs also have been detected in plants (for review, Zhang and Dai, 2022) where they accumulate in response to biotic and abiotic stress (Fan et al., 2020; Wang et al., 2017; Zhang et al., 2020; Zuo et al., 2016). A comparison of

6,519 circRNAs from rice (*Oryza sativa*) with those from 46 other species at the genomic level revealed a high degree of conservation within the Oryza genus (46%) and as much as 8.5% were also found in dicotyledonous plants, showing some conservation of circRNAs in plants (Chu et al., 2022). Of note, an endogenous antisense circRNA was reported to regulate the expression of RuBisCO (Small Subunit Genes) in Arabidopsis (Zhang et al., 2021). Interestingly, circRNAs of *Arabidopsis thaliana* have been detected in leaf intercellular washing fluids (IWF), showing that they are secreted to the plant apoplast. Apoplastic circRNAs were highly enriched in the posttranscriptional modification N6-methyladenine (m6A) (Zand Karimi et al., 2022), which is known to efficiently initiate the translation of circRNAs (Yang et al., 2017). Furthermore, the putative m6A-binding protein GLYCINE-RICH RNA-BINDING PROTEIN 7 (GRP7) and the sRNA-binding protein ARGONAUTE 2 (AGO2) were found in the IWF and coimmunoprecipitated with circRNAs, indicating that these proteins may play a role in the secretion and/or stabilization of apoplastic circRNA.

Knowledge about the molecular mechanism by which circRNAs act in plants is still limited. Nevertheless, artificial circRNAs are promising candidates for agronomical application given that *i.* the structural stability of the circular form is superior to open RNA forms and *ii.* current knowledge suggests their potential multifunctional roles as miRNA sponges and regulators of translation. Here we explore the potential of artificial exogenous circRNAs to target accumulation of an endogenous Green Fluorescence Protein (GFP) reporter protein in Arabidopsis. We show that plant cells treated with the GFP-specific circRNA$_{GFP}$, in contrast to its linear isoform linRNA$_{GFP}$ or a circRNA that does not contain GFP-specific target sequences (circRNACTR$_1$), show reduced GFP accumulation in a sequence- and isoform-specific manner. Moreover, using mutants compromised in DCL and AGO functions, we demonstrate that the circRNA-mediated activity is independent of canonical RNAi pathways. Our report suggest that circRNAs may be developed to novel tools for targeting plant gene expression, opening up new strategies to use designer circRNA for bioherbicide development.

Results

Designing of *GFP*-antisense circRNA

The *ORF* region of a gene is considered a key target for designer antisense circRNAs (Pfafenrot et al. 2021). To develop a potential new tool for targeting plant genes with exogenous RNA, we synthesized circRNA targeting the ORF of a *GFP* reporter gene (Fig. 1A). The exact positions of the antisense sequences were selected based on a secondary structure model of the

ORF (Fig.1B) and mRNA accessibility (Fig. 1C), resulting in an artificial 50 nt antisense circRNA (circRNA$_{GFP}$) that contained an anti-sequence *GFP* sequence of 30 nt with perfect complementarity. As a control for circRNA$_{GFP}$, two different non-specific circRNAs were synthesized, which contained randomized sequences of similar length. The strucures of all circRNAs are shown in Fig. 1D and sequences in Table S1.

Exogenous circRNA$_{GFP}$ reduces GFP accumulation in *GFP*-overexpressing Arabidopsis protoplasts in a sequence-specific manner

We used a protoplast transfection strategy (Wu et al., 2007; Yoo et al., 2007) for the rapid analysis of the putative antisense activity of designer circRNAs. To this end, mesophyll protoplasts isolated from Arabidopsis leaves were co-transfected with 20 μg of plasmid pGY1-35S::GFP (Fig. S1) and 4 μg of the respective circRNA (circRNA$_{GFP}$ and circRNA$_{CTR1}$). The ratio between green GFP fluorescence and red autofluorescence (total protoplasts) was calculated with ImageJ. Upon treatment of protoplasts with circRNA$_{GFP}$, the number of green fluorescent cells was significantly reduced by up to 40% as compared to non-treated or circRNACTR$_1$-treated protoplasts, indicating that circRNA$_{GFP}$ has an inhibitory effect on GFP expression or accumulation and that this effect is sequence-specific (Fig. 2A,B).

To further substantiate this finding, the changes in the amounts of GFP in response to the presence of exogenous circRNAs were quantified upon immunoblotting. Consistent with the above finding, treatment of *GFP*-expressing protoplasts with circRNA$_{GFP}$ reduced the accumulation of GFP in immunoblots by up to 78% compared to non-treated control protoplasts (Fig. 3A).

Inhibition of GFP accumulation by circRNA$_{GFP}$ is independent of DCLs and AGOs

To obtain more information on the mode of action of sequence-specific designer circRNA that reduce GFP accumulation in protoplasts, we tested whether circRNA$_{GFP}$ activity is impaired in Arabidopsis *dcl1-11* and *ago1-27* mutants. Mesophyll protoplasts from *dcl1-11* and *ago1-27* mutants co-transfected with 20 μg plasmid (pGY1-35S::GFP) and 4 μg circRNA showed reduced GFP fluorescence in response to circRNA$_{GFP}$ treatment like wild type Col-0 protoplasts, hinting to the possibility that disruption of AGO1 and DCL1 activities has no effect on circRNA-triggered reduction of GFP accumulation in Arabidopsis protoplasts (Fig. S2, S3).

Consistent with this finding, immunoblot analysis further confirmed reduced GFP accumulation in circRNA$_{GFP}$-treated *dcl1-11* (57%) and *ago1-27* (49%) as well as wild type Col-0 protoplasts (78%) compared to non-treated protoplasts, while the control circRNA$_{CTR1}$ failed to reduce GFP accumulation in protoplasts of both wild type and mutants (Fig. 3B, C). The accumulation of GFP was also reduced in protoplasts derived of *dcl2 dcl3 dcl4* (*dcl2,3,4*) triple mutant plants as well as in protoplasts of *ago2-1* and *ago4-2* mutants (Fig. S4), confirming that the reduced GFP accumulation in response to circRNA$_{GFP}$ is independent of canonical RNAi pathways.

circRNA$_{GFP}$ does not reduce *GFP* transcript abundance

Next we analyzed the effect of circRNA$_{GFP}$ on the transcript level of the *GFP* gene in Arabidopsis protoplasts. To this end, protoplasts were transfected with 20 µg pGY1-35S::GFP plasmid alone or together with either 4 µg circRNA$_{GFP}$ or circRNA$_{CTR1}$, followed by by RT-qPCR measurements of transcript levels at 18 hpt. We found that both circRNAs did not affect GFP transcript levels in wild type protoplasts (Fig. 4A), *dcl1-11* and *ago1-27* protoplasts (Fig. 4B,C) or *dcl2,3,4*, *ago2-1*, and *ago4-1* protoplasts (Fig. S5). These findings suggest that circRNA$_{GFP}$ inhibits protein accumulation in a sequence-specific manner without affecting corresponding transcript levels, through a process that is independent of canonical RNAi pathways.

Sequence-specific inhibition of GFP in protoplasts by circRNA$_{GFP}$ is dose-dependent

To further evaluate and confirm the efficacy of circRNA treatments, we also explored dosis dependence of circRNAs effects on cellular GFP accumulation. The analysis was performed under the same experimental conditions as described above. Wild type Col-0 protoplasts were co-transfected with pGY1-35S::GFP and circRNAs, this time using circRNAs quantities ranging from 1 µg to 8 µg. After 18 h, all samples were inspected by fluorescence microscopy, and GFP fluorescence was quantified with ImageJ. The analysis showed reduced GFP fluorescence in all circRNA$_{GFP}$-treated (Fig. S6A,C), but not in control circRNACTR$_1$ treated (Fig. S6B,C) protoplasts. Moreover, immunoblot analysis showed that the amount of GFP protein was reduced by 30%, 41%, and 44% in protoplasts treated with 2 µg, 4 µg, and 8 µg of circRNA$_{GFP}$, respectively (Fig. 5), indicating that circRNA$_{GFP}$ inhibits GFP protein accumulation in a dose-dependent manner. In contrast, treatment with circRNA$_{CTR1}$ did not significantly reduce GFP protein levels.

The effect of circRNA$_{GFP}$ on GFP accumulation is isoform-specific

Next, we assessed the impact of single-stranded, non-circularized linear antisense RNA (linRNA$_{GFP}$) comprising the same nucleotide sequence and targeting the same *GFP* region as the circRNA$_{GFP}$ on GFP accumulation in immunoblots. Arabidopsis protoplasts were treated with plasmid pGY1-35S::GFP, combined with circular (circRNA$_{GFP}$) or linear (linRNA$_{GFP}$) forms of the GFP antisence RNA, and incubated for 10 h, 18 h, and 32 h. circRNA$_{GFP}$-mediated inhibition of GFP accumulation was already detectable at 10 h, and this effect increased until 32 h of incubation (Fig. 6). In contrast, linRNA$_{GFP}$ showed only a slight initial effect of protein reduction at 10 h, and this inhibitory effect disappeared over time. Altogether, the results show a strong isoform-specific effect of circRNA$_{GFP}$ on GFP accumulation. Hence, our data indicate that circRNAs is superior to corresponding linear RNA in antisense-targeting of plant genes.

Topical application of naked circRNA$_{GFP}$ fails to reduce GFP accumulation in Arabidopsis leaves

While circRNA$_{GFP}$ reduces GFP accumulation in PEG-mediated transfected protoplasts, we wondered whether its topical application on leaves of *GFP*-expressing plants would have a similar effect. To this end, leaves of three-week-old *GFP*-expressing Arabidopsis plants were drop-treated with 10 µg circRNA$_{GFP}$ or circRNA$_{CTR1}$ in 10 µL of ddH_2O. Treated leaves were harvested after 48 h and GFP immunoblot analysis was performed. We found that foliar GFP accumulation was not reduced by circRNA$_{GFP}$ treatment (Fig. S7). Drop-treatment of leaves with 10 µg of 476 bp GFP dsRNA or with 10 µg of 431 bp Clp dsRNA (derived from an intron contained in the *Verticillium longisporum Clp-1* gene; Table S1) as control also did not reduce GFP accumulation (Fig. S7). These results are consistent with the current view that topical application of RNA is unable to interfere with gene expression in intact plants unless adjuvant methods such as pressure spraying or rubbing with abrasives are applied to increase RNA uptake (Dalakouras et al. 2016; 2020).

circRNAs do not induce typical PTI responses such as callose deposition in Arabidopsis leaves

There is growing evidence that dsRNA can activate pattern-triggered immunity (PTI) in plant cells (Niehl et al. 2016; Huang et al. 2023). This is not surprising since dsRNA is produced during virus replication and might be perceived in plants as a PAMP by a pathogen recognition receptor similar to metazoans (Niehl et al. 2016). Upon dsRNA elicitation, plants can activate a battery of immunity-related genes and induce the accumulation of callose at the

plasmodesmata, to avoid viral intercellular movement (Niehl et al. 2016; Huang et al. 2023). We wondered whether circRNAs, with their particular structure, would also trigger PTI responses in Arabidopsis plants. To this end, equal molar amounts of either sequence non-specific circRNAs ($circRNA_{CTR1}$, $circRNA_{CTR2}$), single-stranded linear isoforms of these circRNAs ($linRNA_{CTR1}$, $linRNA_{CTR2}$), synthetic dsRNA analog poly(I:C) (as positive control) or water, were vacuum-infiltrated into Arabidopsis leaf disks together with aniline blue to stain callose. Fluorescence microscopy revealed that poly(I:C) treatment resulted in a strongly brighter aniline blue fluorescence at the plasmodesmata, as compared to the other treatments (Fig. 7A). Quantification of fluorescence showed that poly(I:C) triggered the strongest mean callose intensity. The linear isoform of RNA_{CTR1} ($linRNA_{CTR1}$) also triggered callose deposition, although to a lesser extent (Fig. 7B). Surprisingly, neither of the circRNA molecules induced an increased callose intensity (Fig. 7B). When the concentration of $circRNACTR_2$ was increased by 5 times again no significant callose signal enhancement was observed (Fig. S8). These observations indicate that the treatment of plants with circRNAs does not lead to callose deposition at plasmodesmata. Thus, unlike dsRNA, circRNAs may be able to evade receptor recognition in plants.

Discussion

Apart from the promising undertakings in human medicine (Kim 2022; Zhu et al. 2022), there is growing evidence that different types of RNA molecules can also be used to control plant pests, microbial pathogens and weeds (Banerjee et al., 2017; Baulcombe, 2015; Cai et al., 2018; Koch and Wassenegger, 2021; Mai et al., 2021; Taning et al., 2019; Liu et al., 2020). In agricultural research, strong efforts have been taken to develop non-GMO plant protection measures based on the exogenous application of RNA (SIGS) with some success (Huang et al., 2023; Koch et al., 2016; Niehl et al., 2018; Wang et al., 2016; Zabala-Pardo et al., 2022).

In the context of crop protection, the use of RNA for the targeted control of plant genes offers several potential applications, including its use as herbicide or as antimicrobial agent when targeting plant susceptibility genes (Mai et al., 2021; van Schie et al., 2014). However, the efficiency of exogenous RNA applications such as dsRNA or sRNA so far is hampered by its low stability under agronomic conditions and its weak uptake by leaves (Bennett et al., 2020; Dalakouras et al., 2016; 2020; Liu et al., 2021). Therefore, we wanted to test whether circRNA, in addition to dsRNA, has a potential to be used as a biological agent in agriculture.

We show that exogenous circRNA with antisense sequences to a *GFP* reporter gene (circRNA$_{GFP}$) can reduce GFP protein levels in Arabidopsis protoplasts and that its activity *i.* depends on the topology of the circular isoform as the corresponding linear *GFP* targeting RNA (linRNA$_{GFP}$) had no effect, *ii.* is sequence-specific, as circRNACTR$_1$ lacking the *GFP* antisense sequence is inactive, and *iii.* is independent of RNAi pathways, as protoplasts of various *dcl* and *ago* mutants are indistinguishable from Arabidopsis wild type Col-0 protoplasts in their response to circRNA$_{GFP}$. Isoform- and sequence-specific activity of circRNA was revealed by the reduction in the ratio of green fluorescence vs. total (red) fluorescence in protoplasts treated with the *GFP*-expressing plasmid pGY1-35S::GFP and *GFP* antisense circRNA$_{GFP}$, which was not seen in protoplasts transfected only with plasmid or with plasmid plus non-targeting control circRNA$_{CTR1}$. Consistent with this observation, the immunoblotting assay confirmed that exogenous application of circRNA$_{GFP}$ but not circRNA$_{CTR1}$ or the linear isoform linRNA$_{GFP}$ strongly reduced the abundance of GFP protein by approximately 86% compared to non-treated protoplasts (Fig. 3, Fig. 6). The response of a presentative set of Arabidopsis *dcl* and *ago* mutants including *dcl1-11*, *dcl2,3,4*, *ago1-27*, *ago2-1*, and *ago4-1* furthermore strongly indicates that the reduction of GFP was independent of RNAi pathways.

Consistently, our results showed no significant *GFP* transcript downregulation in the wild type Col-0 protoplasts nor in the *dcl* and *ago* mutants (Fig. 4, Fig. S5). Apparently, circRNA$_{GFP}$ regulated the amount of GFP protein on the translational level in a nucleotide sequence-dependent manner but independent of RNAi. The mechanism might be similar to the blockage-type mechanism induced by circRNA and leading to inhibition of coronavirus Covid-19 proliferation in a cell culture system (Pfafenrot et al., 2021).

The nucleotide sequence-specific antisense activity of circRNA$_{GFP}$ increases over various doses ranging from 1 µg to 8 µg (Fig. 5), where increasing amounts of circRNA$_{GFP}$ showed strong GFP reduction effects of about 30% to 44% (Fig. 5). After 10 hours of protoplast treatment with circRNA$_{GFP}$, we observed a reduction of GFP protein in immunoblots by up to 83% while the isoform linRNA$_{GFP}$ showed a reduction of up to 48% (Fig. 6). Importantly, at later time points, circRNA$_{GFP}$ maintained its strong inhibitory activity on GFP accumulation compared to protoplasts incubated with the control (circRNA$_{CTR1}$), while its linear isoform had no inhibitory effect anymore. Nonetheless, the lasting inhibitory effect of circRNAs is possibly due to the high metabolic stability over linear isoforms, being more resistant to the attack of exonucleases (Alhasan et al. 2016).

GFP protein was reduced in Arabidopsis protoplasts upon PEG-mediated transfection with the pGY1-35S::GFP plasmid and the circRNA$_{GFP}$. Protoplasts lack cell walls and PEG facilitates the entry of plasmid and other nucleic acids into eucaryotic cells (Wu et al. 2009). Topical application of RNA on plant leaves to target plant genes has been more challenging since several barriers (such as plant cuticle and cell wall) need to be overcome (Bennett et al. 2020). In the light of future application of RNA technologies in plant protection, and due to their circular structure and presumed higher stability, we thought it is important to gather first experimental information on the possibility to target GFP accumulation in Arabidopsis leaves via topical application of circRNA. Our results show that topically applied circRNA$_{GFP}$ could not significantly reduce foliar GFP accumulation (Fig. S7), suggesting that other mechanical delivery methods such as high-pressure spray or the use of formulations are needed to facilitate efficient circRNA entry into plant cells (Dalakouras et al. 2020).

There is growing evidence showing that dsRNA induces typical PTI responses in plant cells (Niehl et al. 2016; Huang et al. 2023). Poly(I:C) elicitation triggered callose deposition at the plasmodesmata in Arabidopsis and Nicotiana plants (Huang et al., 2023). In the light of future application of the RNA technology, this has several implications both on the mode of action of RNA pesticides and its approvement by governmental regulation authorities. Therefore, we also wanted to know whether circRNA induces PTI in Arabidpsis leaves. Significantly, incubating leaf disks with the same molarity of poly(I:C), linear, and circular isoforms of RNA molecules let to intriguing results: poly(I:C), as expected, strongly induced callose deposition, while the response to the linear isoform of circRNAs was weaker but still was significantly enhanced for one of them (linRNA$_{CTR1}$) (Fig. 7). In clear contrast, circRNA molecules failed to induce callose deposition (Fig. 7), even when their concentration was increased by 5 times (Fig. S8). Consistent with this finding, a previous study showed that circRNA did not trigger any antiviral response in mammal cells (Breuer et al., 2022). These results highlight the great potential of circRNA to inhibit proteins with high specificity, with little to no side effects.

To date, the use of exogenously applied designer circRNA to target plant gene regulation has not been studied. Therefore, this work paves the way to investigate new approaches of using artificially designed circRNA for a particular antisense function. To recapitulate, our promising findings are that artificially designed circRNA could be used as a new and effective tool for plant gene regulation, just like dsRNA and sRNA, but with a completely different mode of action. In this way, our work will initiate further future research on circRNA applications, with

the aim to modulate expression of plant endogous genes, and to develop new RNA-based herbicides and antimicrobial compounds.

Materials and methods

Plant material and isolation of Arabidopsis protoplasts

Arabidopsis thaliana (Col-0) wild type (WT) and the mutants *ago1-27*, *ago2-1*, *ago4-1*, *dcl1-11* and triple mutant *dcl2,3,4* were obtained from NASC (https://arabidopsis.info/). All mutants were verified by genotyping. *A. thaliana* plants constitutively expressing *GFP* were published in Harvey et al., (2020). Mesophyll protoplasts were produced using the tape-Arabidopsis-sandwich method (Wu et al., 2007) starting from leaves of 30-day-old plants grown at 22°C/18°C (day/night cycle) with 60% relative humidity and a photoperiod of 8/16 h (240 µmol m^{-2} s^{-1} photon flux density) in a soil combination of type-T (F.-E. Typ Nullerde, Hawita) and sand with a ratio of 3:1. Protoplasts were enzymatically released from leaves in an enzymatic solution containing 0.4 M mannitol, 20 mM KCl, 20 mM MES, pH 5.7, 1% (w/v) cellulase R10, and 0.25% (w/v) macerozyme R10 (Duchefa Biochemie B.V.). Before use, the enzyme solution was heated to 55°C for 10 min to solubilize the enzymes, and then 10 mM $CaCl_2$ and 0.2% BSA were added. Finally, the solution was filter sterilized with a 45 µm filter (Merck SA). Ten to 15 leaves with the upper epidermis peeled off were shaken (50-60 rpm) in the activated enzyme solution for 1 h in the dark. Subsequently, protoplasts were collected by filtration through a nylon mesh and centrifuged at 100x g at 4°C. The final concentration of mesophyll protoplasts used in each experiment was 500,000/mL.

Design of circRNAs

The structure model of all circRNAs and structures were predicted with mRNA structure were predicted with mfold (version 3.6, mfold_util 4.7 and RNA Folding Form V2.3; www.unafold.org; Waugh et al. 2002; Zuker, 2003) and RNAfold (RNAfold web server, university of Vienna), respectively. The 30 nt antisense target sequence for the *GFP* gene (contained in the pGY1-35S::GFP plasmid; Schweizer et al., 1999) in the 50 nt $circRNA_{GFP}$ was retrieved from the *GFP-ORF* region. mRNA accessibility was assessed with the software RNAup (Vienna RNA Package, http://rna.tbi.univie.ac.at/). As a control for $circRNA_{GFP}$, two non-specific circRNAs were produced, which contain a randomized 25 nt or 46 nt sequence and a 20 nt backbone, forming a 45 nt $circRNA_{CTR1}$ and 66 nt $circRNA_{CTR2}$, respectively.

circRNA design and synthesis were performed as described (Nielsen et al., 2022; Pfafenrot et al., 2021). Briefly, the antisense sequences were inserted between two spacers consisting of three unrelated nucleotides between the constant backbone, and this arrangement assured the stem-loop formation in both the antisense and control sequences. The sequences of oligonucleotides including the T7 promoter were commercially synthesized (Sigma-Aldrich). Subsequently, these were annealed to produce templates suitable for *in-vitro* transcription.

Production of circRNAs, linRNAs and dsRNAs

circRNAs were produced by *in-vitro* transcription from annealed DNA oligonucleotide templates (Table S2) using HighScribe T7 high-yield RNA synthesis kit (NEB) along with ATP, CTP, UTP, GTP (7.5 mM each), GMP (30 mM, Merck), and RNaseOut (Thermo Fisher Scientific) at 37°C for 2 h. Before transcription, the template DNA was digested with RQ1DNase (Promega) at 37°C for 30 min. Transcripts were purified with a Monarch RNA purification kit (NEB) and quantified with a Qubit™ RNA broad-range assay kit (Thermo Fisher Scientific). The RNA was circularized overnight at 16°C with 200 U of T4 RNA ligase (Thermo Fisher Scientific) in 200 µl T4 RNA ligase buffer containing 0.1 mg/mL BSA and RNaseOut (Thermo Fisher Scientific). Following this reaction, the circRNA was cleaned by phenol/chloroform extraction (Roth) and ethanol precipitation. Single-stranded linear RNA (linRNA) with the same nt sequence was produced the same way but without circularization. Both linRNA and circRNAs were further gel-purified from denaturing polyacrylamide gels as described (Breuer and Rossbach, 2020). To confirm the circularity of circRNAs, 250 ng of circRNA or linRNA were treated with or without 2 U of RNase R enzyme for 25 min at 37°C (Biozym) and analyzed by denaturing polyacrylamide gel electrophoresis followed by ethidium bromide staining.

dsRNA was produced *in-vitro* with MegaScript T7 Transcription Kit Plus (ThermoFisher). Sequences are shown in Table S1. Primers are listed in Table S2.

Treatment of protoplasts with circRNAs and linRNAs

circRNA (or the respective linRNA) together with 20 µg of plasmid pGY1-35S::GFP in a total volume of 20 µL were added to 1×10^5 mesophyll protoplasts in 200 µL MMg buffer (0.4 M mannitol, 15 mM $MgCl_2$, 4 mM MES, pH 5.7) under gentle pipetting. Then 220 µL of PEG-Ca^{2+} (40% PEG-4000, 0.2 M mannitol, 0.1 M $CaCl_2$) were slowly added to the protoplast suspension and incubated at room temperature (Yoo et al. 2007). After 15 min of incubation, the protoplasts were washed by centrifugation two times with the W5 buffer (154 mM NaCl,

125 mM $CaCl_2$, 5 mM KCl, 2 mM MES, pH 5.7). Subsequently, protoplasts (500,000 / mL) were resuspended in W1 buffer (0.5 M mannitol, 20 mM KCl, 4 mM MES, pH 5.7) and incubated in the dark at 25°C. After 18 h, protoplasts were inspected under the fluorescence microscope (MZ16F Leica, Germany) and at least three pictures were taken from the same treatment at different spots. Fluorescence was measured from these pictures by using ImageJ free software (https://imagej.net/ij/) and the ratio of fluorescence levels between the GFP fluorescent protoplasts (λ_{exc} 470, λ_{em} 525 nm) and total protoplasts (red autofluorescence from the chlorophyll, λ_{exc} 480, λ_{em} 510 nm) was calculated.

Drop-treatment of intact plants with circRNAs and dsRNAs

Three-week-old *GFP*-expressing *A. thaliana* plants were used for the topical applications of circRNAs and dsRNAs. All circRNAs and dsRNAs were eluted in Milli-Q water. 22 µL drops containing 10 µg of dsRNA or 10 µL drops containing 10 µg circRNA were applied onto the upper leaf surface with the help of a pipette, without mechanical wounding, and left for uptake in the climate chamber with the conditions described above. After the time points indicated in the figure legends, leaves were collected for protein extraction and further analysis by immunoblotting.

Plant materials and growth conditions for callose deposition assay, callose staining

A. thaliana Col-0 plants were grown in soil and kept in a growth chamber equipped with LED lights under 12h/12h light/dark periods at 22°C/18°C. Arabidopsis leaf disks were excised using a cork borer and incubated overnight in 1 mL of distilled water in the same chamber where the plants were grown. Leaf disks were then washed two times with distilled water, placed on microscope slides, and covered with coverslips fixed with tape. The leaf disks were treated with 200 µL of a 0.1% aniline blue solution (pH=9) containing either water, 500 ng/µL of poly(I:C) (Sigma-Aldrich, USA) or either 50 ng/µL or 250 ng/µL of $circRNA_{CTR}$ (circular or linear versions) by adding the respective solution to the space between the slide and the coverslip and by evacuation for 2 min (0.08 MPa). After incubation in the dark for 30 min the callose staining at epidermal plasmodesmata was imaged with a Zeiss LSM 780 confocal laser scanning microscope equipped with ZEN 2.3 software (Carl Zeiss, Jean, Germany) by applying a 405 nm diode laser for excitation and filtering the emission at 475-525 nm. 8-bit images acquired with a 40× 1.3 N.A. Plan Neofluar objectives with oil immersion were analyzed with ImageJ software (https://imagej.net/ij/) using the plug-in calloseQuant (Huang et al., 2022). The

fluorescence intensity levels of the callose spots were measured in 3-4 images taken from each leaf disk. Three leaf disks from three different plants were analyzed per condition. Normal distribution of the data was estimated and differences in p-values between treatments and the control (water) were determined by parametric one-way ANOVA followed by Dunnett's multiple comparisons test.

Protein isolation, gel blot, and imaging analysis

Protein extraction from protoplasts was performed using 4x SDS buffer (1 M Tris HCl, pH 6.8, 80% glycerol (v:v), Bromophenol Blue 10 mg, 4% SDS (w:v), 1 M of dithiothreitol (DTT) in 20 ml Milli-Q water). The sample was vortexed, short centrifuged, and heated to 95°C for 5 min and then centrifuged at 12,500 rpm for 2 min at 4°C. Protein concentration in the supernatant was determined according to the Bradford Ultra method (Bradford, 1976) on a Bio-Spectrophotometer (Eppendorf) at 595 nm. Then, 4 µg of each protein sample was loaded onto a 12.5 % SDS-PAGE gel. The built-in software from the ChemiDoc MP imaging system (Bio-Rad) was used to evaluate protein band intensity in all western blots. Band intensity of control plants was set to one, and protein accumulation was calculated as a ratio between GFP and Actin. The protoplast counting for all the samples was done by ImageJ analysis.

RNA isolation and gene expression analysis

Total RNA was extracted with the Direct-zol™ RNA Microprep kit (Zymo Research) and treated with DNAsse I following the manufacturer's instructions. 1 µg of RNA was used for cDNA synthesis using a cDNA kit (RevertAid RT Kit, Thermo Fischer Scientific). 30 ng of the cDNA were used for RT-qPCR analysis (QuantStudio 5 Real-Time PCR system; Applied Biosystems). Ct values were analyzed with QuantStudio design and analysis software (Applied Biosystems). Transcript quantities were determined by using the $2^{-\Delta\Delta Ct}$ method (Livak and Schmittgen, 2001), which normalizes measured transcript levels to the levels of a reference transcript (*Ubiquitin*). The primer pairs employed for expression analysis are listed in Table S1.

Statistical analysis

The statistitical significance between sets of parametric data was analyzed with either one sample Student's t-test, or one-way ANOVA followed by Dunnett's post-hoc test, whereas the one sample Wilcoxon test and Kruskal-Wallis tests were used for non-parametric sets. A

description of the specific tests is given in figure legends. Callose quantification experiments were repeated twice with similar outcomes. All the other experiments were repeated at least three times.

Acknowledgment

This work was funded by ERA-NET SusCrop 2 and the Deutsche Forschungsgemeinschaft (DFG) to KHK (RU5116), and by ERA-NET SusCrop 2 and the Agence National de la Recherche (ANR) to MH (ANR-21-SUSC-0003-01; ANR-21-CE20-0020-01).

Legends to Figures

Figure 1: Nucleotide sequences and topology of designer circRNAs and their target sequences in the *GFP* gene. (A) *GFP*-ORF region nucleotide sequence with color code: the 30 nt target sequence of the 50 nt *GFP* antisense circRNA$_{GFP}$ is highlighted in red. Highlighted in blue, the CaMV35S promotor sequence; highlighted in yellow, the 5'UTR; red font represents the circRNA target sequence (30 nt); ATG underligned in green, start codon; TAA underligned in red, stop codon; highlighted in green, the 3'UTR; terminator sequence highlighted in grey. (B) *GFP* mRNA secondary structure, red box indicates the antisense circRNA target region. (C) *GFP* mRNA accessibility, determined with the program RNAup (Vienna RNA Package, http://rna.tbi.univie.ac.at/). The *GFP* mRNA sequence (5'UTR and 3'UTR included) was used with its own antisense RNA sequence to determine RNA accessibility. This analysis served as a guide for selecting sequence sections for antisense circRNA design. Green box describes the sequence of the antisense circRNA$_{GFP}$. (D) The secondary structure of designer circRNAs was determined with the program mfold (www.unafold.org; Zuker 2003). The *GFP* target sequence is colored in green, while randomized control sequences are colored in blue.

Figure 2: Imaging analysis of GFP accumulation in Arabidopsis WT protoplasts 18 hours after transfection. Protoplasts were transfected with 20 µg pGY1-35S::GFP plasmid alone or with plasmid and 4 µg of *GFP* antisense circRNA$_{GFP}$, or with plasmid and 4 µg non-targeting circRNA$_{CTR1}$ as control. (A) After 18 h, protoplasts were inspected under the fluorescence microscope using two different filters to calculate the ratio in fluorescence levels between the GFP fluorescent protoplasts (λ_{exc} 470, λ_{em} 525 nm) and total protoplasts (red autofluorescence

from the chlorophyll, λ_{exc} 480, λ_{em} 510 nm). Fluorescence was measured based on pictures by using ImageJ software. (B) Depicted is the ratio between green pixels (GFP fluorescence) and red pixels (total protoplasts chlorophyll fluorescence) as calculated with ImageJ. Bars represent the average of the measurements of at least 3 pictures taken at different spots with standard error of the mean (SEM). Statistical analysis was performed with one-way ANOVA, where * denotes $p \leq 0.05$ significance vs. control protoplasts (Dunnett's test).

Figure 3: Immunoblot analysis of the accumulation of GFP in Arabidopsis mesophyll protoplasts from wild type Col-0 (A) and RNAi mutants *dcl1-11* (B) and *ago1-27* (C) upon treatment with *GFP* antisense $circRNA_{GFP}$ and non-targeting $circRNACTR_1$. Protoplasts were transfected with 20 µg of pGY1-35S::GFP plasmid alone or with a mixture of plasmid plus 4 µg of $circRNA_{GFP}$ and $circRNA_{CTR1,}$ respectively. Equal amounts of protein were analyzed by immunoblotting, using Arabidopsis actin visualized with an anti-Actin anitibody as a loading control. The ratio of GFP accumulation is indicated below the bands (expressed as ratio between GFP and actin signals).

Figure 4: RT-qPCR analysis of the amount of *GFP* transcripts in Arabidopsis mesophyll protoplasts from WT (A), and RNAi mutants *dcl1-11* (B) and *ago1-27* (C) upon treatment with *GFP* antisense $circRNA_{GFP}$ and non-targeting control $circRNACTR_1$. Protoplasts were transfected with 20 µg of pGY1-35S::GFP plasmid alone or with a mixture of plasmid plus 4 µg of $circRNA_{GFP}$ and $circRNA_{CTR1,}$ respectively. Relative *GFP* expression was measured after 18 h of treatment. Values were normalized to the housekeeping gene *Ubiquitin*. Bars represent an average of three independent biological experiments with standard error of the mean (SEM). No statistical significant differences between treatments and genotypes were detected (one sample t-test, $p \geq 0.05$).

Figure 5: Dose dependence of GFP accumulation in Arabidopsis protoplasts after treatment with increasing concentrations of circRNAs. Protoplasts were transfected with 20 µg plasmid pGY1-35S::GFP alone or with a mixture of plasmid and increasing amounts of $circRNA_{GFP}$ and $circRNA_{CTR1}$ for 18 h. The values below the GFP signal indicate the remaining amount of GFP protein in percent. An anti-Actin antibody was used to visualize Actin as an internal loading control. The ratio of GFP protein accumulation modification is indicated below the bands (expressed as ratio between GFP and actin signals).

Figure 6: Immunoblot analysis of GFP accumulation in Arabidopsis protoplasts after treatment with the *GFP* antisense circRNA$_{GFP}$ and its corresponding linear isoform linRNA$_{GFP}$. Protoplasts were transfected with pGY1-35S::GFP alone or with a mixture of the plasmid and either circRNA$_{GFP}$ or linRNA$_{GFP}$ and analysed for GFP accumulation after 10 h (A), 18 h (B) and 32 h (C). An anti-Actin antibody was used to visualize Actin as a loading control. GFP reduction is indicated below the band as percentage of GFP in the control protoplasts. The ratio of GFP protein accumulation modification is indicated below the bands (expressed as ratio between GFP and actin signals).

Figure 7: Treatment with designer circRNA does not trigger callose deposition at plasmodesmata in Arabidopsis leaves. (A) Callose accumulation at plasmodesmata (PD) upon staining with aniline blue. Samples were treated with aniline blue and water (negative control), 500 ng/µL of poly(I:C) (positive control), or 50 ng/µL of two isoform of non-targeting sequences, depicted as linRNA$_{CTR1}$ and circRNA$_{CTR1}$ respectively; or 50 ng/µL of linear and circular forms of RNA$_{CTR2}$ (linRNA$_{CTR2}$ and circRNA$_{CTR2}$, respectively). For a better visualization, color was assigned to the 8-bit images by applying the "fire" look-up table using the Image J software. Scale bar, 10 µm. (B) Mean values of callose intensity levels at PD in individual images taken of epidermal cells of leaf disks treated with a 0.1% aniline blue solution containing water, 500 ng/µL of poly(I:C), or 50 ng/µL of either linRNA or circRNA. Error bars show the standard error of the mean. Parametric mean value variances were tested by one-way ANOVA followed by Dunnett's multiple comparisons test. ****, $p \leq 0.0001$; *, $p \leq 0.05$; ns, non-significant.

Supplementary data and figure legends

Figure S1: Plant protoplast transfection plasmid pGY1-35S::GFP. The length of the total plasmid backbone is 4,238 bp, consisting of a strong constitutive *Cauliflower Mosaic Virus* 35S (CaMV35S) promoter and terminator. The whole construct confers resistance to ampicillin and carbenicillin antibiotics. *GFP* is inserted and its expression is under the control of CaMV promoter and terminator. The Map was generated by SnapGene freeware (https://en.freedownloadmanager.org/Windows-PC/SnapGene-Viewer-FREE.html.

Figure S2: Imaging analysis of GFP accumulation in Arabidopsis *dcl1-11* protoplasts 18 hours after transfection. Protoplasts were transfected with 20 µg of plasmid pGY1-35S::GFP alone or with plasmid and 4 µg of *GFP* antisense circRNA$_{GFP}$, or with plasmid and 4 µg non-targeting circRNA$_{CTR1}$ as control.. (A) After 18 h, protoplasts were inspected under the fluorescence microscope using two different filters to calculate the ratio in fluorescence levels between the GFP fluorescent protoplasts (λ_{exc} 470, λ_{em} 525 nm) and total protoplasts (red autofluorescence from the chlorophyll, λ_{exc} 480, λ_{em} 510 nm). Fluorescence was measured based on pictures using ImageJ software. (B) Depicted is the ratio between green pixels (GFP fluorescence) and red pixels (total protoplasts chlorophyll fluorescence) as calculated with ImageJ. Bars represent the average of the measurements of at least 3 pictures taken at different spots with standard error of the mean (SEM). Statistical analysis was performed with one-way ANOVA, where * denotes $p \leq 0.05$ significance vs. control protoplasts (Dunnett's test).

Figure S3: Imaging analysis of GFP accumulation in Arabidopsis *ago1-27* protoplasts 18 hours after transfection. Protoplasts were transfected with 20 µg of plasmid pGY1-35S::GFP alone or with plasmid and 4 µg of *GFP* antisense circRNA$_{GFP}$, or with plasmid and 4 µg non-targeting circRNA$_{CTR1}$ as control.. (A) After 18 h, protoplasts were inspected under the fluorescence microscope using two different filters to calculate the ratio in fluorescence levels between the GFP fluorescent protoplasts (λ_{exc} 470, λ_{em} 525 nm) and total protoplasts (red autofluorescence from the chlorophyll, λ_{exc} 480, λ_{em} 510 nm). Fluorescence was measured based on pictures using ImageJ software. (B) Depicted is the ratio between green pixels (GFP fluorescence) and red pixels (total protoplasts chlorophyll fluorescence) as calculated with ImageJ. Bars represent the average of the measurements of at least 3 pictures taken at different spots with standard error of the mean (SEM). Statistical analysis was performed with one-way ANOVA, where * denotes $p \leq 0.05$ significance vs. control protoplasts (Dunnett's test).

Figure S4: Immunoblot analysis of the accumulation of GFP in Arabidopsis mesophyll protoplasts from RNAi mutants *dcl2,3,4*, *ago2-1* and *ago4-1* upon treatment with *GFP* antisense circRNA$_{GFP}$ and non-targeting circRNACTR$_1$. Protoplasts were transfected with 20 µg of pGY1-35S::GFP plasmid alone or with a mixture of plasmid plus 4 µg of circRNA$_{GFP}$ and circRNA$_{CTR1,}$ respectively. Equal amounts of protein were analyzed by Ponceau-S staining.

Figure S5: RT-qPCR analysis of the amount of *GFP* transcripts in Arabidopsis mesophyll protoplasts from RNAi mutants *dcl2,3,4* (A), *ago2-1* (B), and *ago4-1* (C) upon treatment with

GFP antisense circRNA$_{GFP}$ and non-targeting control circRNACTR$_1$. Protoplasts were transfected with 20 µg of pGY1-35S::GFP plasmid alone or with a mixture of plasmid plus 4 µg of circRNA$_{GFP}$ and circRNA$_{CTR1,}$ respectively. Relative *GFP* expression was measured after 18 h of treatment. Values were normalized to the housekeeping gene *Ubiquitin*. Bars represent an average of three independent biological experiments with standard error of the mean (SEM). No statistical significant differences between treatments and genotypes were detected (one sample t-test for (A) and (C) and one sample Wilcoxon test for (B), $p \geq 0.05$).

Figure S6: Dose-response imaging analysis of GFP accumulation in Arabidopsis WT protoplasts 18 hours after transfection. Protoplasts were transfected with 20 µg of plasmid pGY1-35S::GFP alone or with plasmid and the indicated amount of non-targeting circRNACTR$_1$ (A) or *GFP* antisense circRNA$_{GFP}$ (B), respectively. After 18 h, protoplasts were inspected under the fluorescence microscope using two different filters to calculate the ratio in fluorescence levels between the GFP fluorescent protoplasts (λ_{exc} 470, λ_{em} 525 nm) and total protoplasts (red autofluorescence from the chlorophyll, λ_{exc} 480, λ_{em} 510 nm). Fluorescence was measured based on pictures by using ImageJ free software. (C) Depicted is the ratio between green pixels (GFP fluorescence) and red pixels (total protoplasts chlorophyll fluorescence) as calculated with ImageJ. Bars represent the average of the measurements of at least 3 pictures taken at different spots with standard error of the mean (SEM). Statistical analysis was performed with one-way ANOVA, where asterisks indicate statistical significance of the group to the control group (*$p \leq 0.05$; **$p \leq 0.01$; ***$p \leq 0.001$; Dunnett's test).

Figure S7: Topical application of designer circRNAs on leaves of constitutively *GFP*-expressing Arabidopsis plants. Three-week-old leaves were drop-inoculated with 10 µg of *GFP* antisense circRNA$_{GFP}$, non-targeting control circRNA$_{CTR1}$, and two dsRNAs, *GFP*-targeting 476 nt dsRNA$_{GFP}$ and non-targeting control 431 nt dsRNA$_{Clp}$. After 48 h, samples were harvested for immunoblotting analysis. An anti-Actin antibody was used to visualize Actin as a loading control. The percentage of GFP reduction is indicated below the band (referred as pertentage of the GFP in control protoplasts). The ratio of GFP protein accumulation modification is indicated below the bands (expressed as ratio between GFP and actin signals).

Figure S8: Mean values of callose intensity levels at PD in individual images taken of epidermal cells of leaf disks treated with a 0.1% aniline blue solution containing water (control), 500 ng/µL of poly(I:C), or either 50 ng/µL or 250 ng/µL of circRNA$_{CTR2}$. Error bars show the

standard error of the mean. Parametric mean value variances were tested by one-way ANOVA followed by Dunnett's multiple comparisons test. ***, $p \leq 0.001$; ns = non-significant.

Table S1: Nucleotide sequence of circRNAs and dsRNAs used in this study.

Table S2: List of oligonucleotides used in this study.
Oligonucleotides are used for circRNA and dsRNA production, as well as for RT-qPCR.

References

Banerjee S, Banerjee A, Gill SS, Gupta OP, Dahuja A, Jain PK, and Sirohi A. (2017) RNA Interference: A Novel Source of Resistance to Combat Plant Parasitic Nematodes. Front Plant Sci. 8:834. doi: 10.3389/fpls.2017.00834.

Baulcombe, D.C., (2015) VIGS, HIGS and FIGS: small RNA silencing in the interactions of viruses or filamentous organisms with their plant hosts. Current Opinion in Plant Biology 26, 141-146,

Baulcombe, D.C. (2004) RNA silencing in plants. Nature 431, 356–363.

Bennett, M., Deikman, J, Hendrix, B, Iandolino, A (2020) Barriers to efficient foliar uptake of dsRNA and molecular barriers to dsRNA activity in plant cells. Frontiers in Plant Science 11. DOI=10.3389/fpls.2020.00816

Bradford, M.M. (1976) A rapid and sensitive method for the quantitation of microgram quantities of protein utilizing the principle of protein-dye binding. Analytical Biochemistry, 72(1-2), 248-254.

Breuer, J., and Rossbach, O. (2020). Production and purification of artificial circular RNA sponges for application in molecular biology and medicine. Methods and protocols, 3(2), 42.

Breuer, J, Barth, P, Noe, Y, Shalamova L, Goesmann, A, Weber, F, Rossbach, O. (2022) What goes around comes around: Artificial circular RNAs bypass cellular antiviral responses. Mol Ther Nucleic Acids. 28:623-635. doi: 10.1016/j.omtn.2022.04.017.

Buck, A., Coakley, G., Simbari, F. et al.. (2014) Exosomes secreted by nematode parasites transfer small RNAs to mammalian cells and modulate innate immunity. Nat. Commun. 5, 5488.

Cai, Q., He, B., Kogel, K.H., and Jin, H. (2018). Cross-kingdom RNA trafficking and environmental RNAi-nature's blueprint for modern crop protection strategies. Current opinion in microbiology, 46, 58-64.

Chen, A., Halilovic, L., Shay, J.H., Koch, A., Mitter, N., and Jin, H. (2023) Improving RNA-based crop protection through nanotechnology and insights from cross-kingdom RNA trafficking. Curr Opin Plant Biol. 102441. doi: 10.1016/j.pbi.2023.102441.

Chu, Q., Ding, Y., Xu, X., Ye C-Y., Zhu, Q-H.,Guo, L., and Fan, L. (2022). Recent origination of circular RNAs in plants. New Phytologist 233: 515-525

Cocquerelle, C., Mascrez, B., Hétuin, D., and Bailleul, B. (1993) Mis-splicing yields circular RNA molecules. The FASEB Journal, 7(1), 155-160.

Dalakouras, A., Wassenegger, M., McMillan, J.N., Cardoza, V., Maegele, I., Dadami, E., Runne, M., Krczal, G., and Wassenegger, M. (2016) Induction of Silencing in Plants by High-Pressure Spraying of In vitro-Synthesized Small RNAs. Frontiers in Plant Science 7.

Dalakouras, A., Wassenegger, M., Dadami, E., Ganopoulos, I., Pappas, M.L., and Papadopoulou, K. (2020) Genetically Modified Organism-Free RNA Interference: Exogenous Application of RNA Molecules in Plants. Plant Physiol. 182(1):38-50. doi: 10.1104/pp.19.00570.

Deguine, JP., Aubertot, JN., Flor, R.J. et al. (2021) Integrated pest management: good intentions, hard realities. A review. Agron. Sustain. Dev. 41, 38.

Fan, J., Quan, W., Li, G. B., Hu, X. H., Wang, Q., Wang, H., et al. (2020) circRNAs are involved in the rice-Magnaporthe oryzae interaction. Plant Physiology, 182(1), 272-286.

Fire, A., Xu, S., Montgomery, M. K., Kostas, S. A., Driver, S. E., & Mello, C. C. (1998) Potent and specific genetic interference by double-stranded RNA in *Caenorhabditis elegans*. Nature, 391(6669), 806-811.

Fletcher, S.J., Reeves, P.T., Hoang B.T., Mitter, N. (2020) A perspective on RNAi-based biopesticides. Frontiers in Plant Science 11; DOI=10.3389/fpls.2020.00051.

Ghildiyal, M. and Zamore, P. D. (2009) Small silencing RNAs an expanding universe. Nat. Rev. Genet. 10, 94–108.

Guo, J.U., Agarwal, V., Guo, H., and Bartel, D.P. (2014) Expanded identification and characterization of mammalian circular RNAs. Genome Biology, 15(7), 1-14.

Hansen, T.B., Jensen, T.I., Clausen, B.H., Bramsen, J.B., Finsen, B., Damgaard, C.K., and Kjems, J. (2013) Natural RNA circles function as efficient microRNA sponges. Nature, 495(7441), 384-388.

Harvey, S., Kumari, P., Lapin, D., Griebel, T., Hickman, R. et al., (2020) Downy Mildew effector HaRxL21 interacts with the transcriptional repressor TOPLESS to promote

pathogen susceptibility. PLOS Pathogens 16(8): e1008835. doi.org/10.1371/journal.ppat.1008835.

He, A. T., Liu, J., Li, F., and Yang, B.B. (2021) Targeting circular RNAs as a therapeutic approach: current strategies and challenges. Signal transduction and targeted therapy, 6(1), 185.

Hsu, M.T., and Coca-Prados, M. (1979) Electron microscopic evidence for the circular form of RNA in the cytoplasm of eukaryotic cells. Nature, 280(5720), 339-340.

Huang, C., Mutterer, J., and Heinlein, M. (2022) In vivo aniline blue staining and semi-automated quantification of callose deposition at plasmodesmata Methods Mol Biol 2457, 151-165.

Huang, C., Sede, A.R., Elvira-González, L., Yan, Y., Rodriguez, M.E., Mutterer, J., Emmanuel, E., Shan, L., and Heinlein, M. (2023) dsRNA-induced immunity targets plasmodesmata and is suppressed by viral movement proteins, The Plant Cell, 35(10), 3845–3869, doi.org/10.1093/plcell/koad176.

IPPC Secretariat, (2021) Scientific review of the impact of climate change on plant pests – A global challenge to prevent and mitigate plant pest risks in agriculture, forestry and ecosystems. Rome. FAO on behalf of the IPPC Secretariat. https://doi.org/10.4060/cb4769en

Jeck, W.R., and Sharpless, N.E. (2014) Detecting and characterizing circular RNAs. Nature biotechnology, 32(5), 453–461. https://doi.org/10.1038/nbt.2890

Jeck, W. R., Sorrentino, J. A., Wang, K., Slevin, M. K., Burd, C. E., Liu, J., et al. (2013) Circular RNAs are abundant, conserved, and associated with ALU repeats. Rna, 19(2), 141-157.

Khajuria, C., Ivashuta, S., Wiggins, E., Flagel, L., Moar, W., Pleau, M., Miller, K., Zhang, Y., Ramaseshadri, P., Jiang, C., and Hodge, T. (2018) Development and characterization of the first dsRNA-resistant insect population from western corn rootworm, Diabrotica virgifera virgifera LeConte. PloS one. 13(5):e0197059.

Kim, Y.K. (2022) RNA therapy: rich history, various applications and unlimited future prospects. Exp Mol Med. 54(4):455-465. doi: 10.1038/s12276-022-00757-5.

Koch, A., Biedenkopf, D., Furch, A., Weber, L., Rossbach, O., Abdellatef, E., Linicus, L., Johannsmeier, J., Jelonek, L., Goesmann, A., Cardoza, V., McMillan, J., Mentzel, T., and Kogel, K.H. (2016) An RNAi-Based Control of Fusarium graminearum Infections Through Spraying of Long dsRNAs Involves a Plant Passage and Is Controlled by the

Fungal Silencing Machinery. PLOS Pathogens, 12(10), e1005901–e1005901. https://doi.org/10.1371/journal.ppat.1005901

Koch, A. and Wassenegger, M. (2021) Host-induced gene silencing – mechanisms and applications. New Phytol. 231: 54-59. doi.org/10.1111/nph.17364.

Köhl, J., Booij, K., Kolnaar, R. et al. (2019) Ecological arguments to reconsider data requirements regarding the environmental fate of microbial biocontrol agents in the registration procedure in the European Union. BioControl 64, 469–487. https://doi.org/10.1007/s10526-019-09964-y

Kremer R.J. (2023) Chapter 7 - Bioherbicide development and commercialization: challenges and benefits, Editor(s): Opender Koul, Development and Commercialization of Biopesticides, Academic Press, Pages 119-148, ISBN 9780323952903.

Kulkarni, J. A., Witzigmann, D., Thomson, S. B., Chen, S., Leavitt, B. R., Cullis, P. R., and van der Meel, R. (2021) The current landscape of nucleic acid therapeutics. Nature Nanotechnology, 16(6), 630-643.

Lamichhane, J.R., Dachbrodt-Saaydeh, S., Kudsk, P., Messéan, A. (2016) Toward a reduced reliance on conventional pesticides in European agriculture. Plant Disease 100(1): 10-24.

LaMonte, G., Philip, N., Reardon, J., Lacsina J.R., Majoros, W., Chapman, L, Thornburg, CD, Telen, M.J., Ohler, U., Nicchitta, C.V., Haystead, T., Chi, J.T. (2012) Translocation of sickle cell erythrocyte microRNAs into Plasmodium falciparum inhibits parasite translation and contributes to malaria resistance. Cell Host Microbe 12(2):187-99. doi: 10.1016/j.chom.2012.06.007.

Livak, K.J. and Schmittgen, T.D. (2001) Analysis of Relative Gene Expression Data Using Real-Time Quantitative PCR and the 2-ΔΔCT Method. Methods, 25, 402-408. http://dx.doi.org/10.1006/meth.2001.1262

Liu, S., Ladera-Carmona, M.J., Poranen, M.M. et al. (2021) Evaluation of dsRNA delivery methods for targeting macrophage migration inhibitory factor MIF in RNAi-based aphid control. J. Plant Dis. Prot. 128, 1201–1212). https://doi.org/10.1007/s41348-021-00464-9

Liu, S., Jaouannet, M., Dempsey, D.A., Imani, J., Coustau, C., and Kogel, K.H. (2020) RNA-based technologies for insect control in plant production. Biotechnol Adv. 39:107463. doi: 10.1016/j.biotechadv.2019.107463.

Mai, J., Liao, L., Ling, R., Guo, X., Lin, J., Mo, B., Chen, W., and Yu, Y. (2021) Study on RNAi-based herbicide for Mikania micrantha. Synthetic and Systems Biotechnology 6(4), 437-445.

Memczak, S., Jens, M., Elefsinioti, A., Torti, F., Krueger, J., Rybak, A., et al., (2013) Circular RNAs are a large class of animal RNAs with regulatory potency. Nature, 495(7441), 333-338.

Mishra, S., Dee, J., Moar, W. et al. (2021) Selection for high levels of resistance to double-stranded RNA (dsRNA) in Colorado potato beetle (Leptinotarsa decemlineata Say) using non-transgenic foliar delivery. Sci Rep 11, 6523 (2021). https://doi.org/10.1038/s41598-021-85876-1

Mitter, N., Worrall, E.A., Robinson, K.E., Li P., Jain, R.G., Taochy C., Fletcher, S.J., Carroll, B.J., Lu, G.Q., and Xu, Z.P. (2017) Clay nanosheets for topical delivery of RNAi for sustained protection against plant viruses. Nat Plants. 3:16207. doi: 10.1038/nplants.2016.207.

Niehl, A., Soininen, M., Poranen, M.M. and Heinlein, M. (2018) Synthetic biology approach for plant protection using dsRNA. Plant Biotechnol J, 16: 1679-1687. https://doi.org/10.1111/pbi.12904

Niehl, A., Wyrsch, I., Boller, T. and Heinlein, M. (2016), Double-stranded RNAs induce a pattern-triggered immune signaling pathway in plants. New Phytol, 211: 1008-1019. doi.org/10.1111/nph.13944.

Nielsen, A.F., Bindereif, A., Bozzoni, I., Hanan, M., Hansen, T. B., Irimia, M., et al., (2022) Best practice standards for circular RNA research. Nature methods, 19(10), 1208-1220.

Pareek, A, Dhankher O.P., and Foyer C.H. (2020) Mitigating the impact of climate change on plant productivity and ecosystem sustainability. Journal of Experimental Botany, 71(2), 451–456, https://doi.org/10.1093/jxb/erz518

Perez-Alvarez, R., Nault, B.A. & Poveda, K. (2019) Effectiveness of augmentative biological control depends on landscape context. Sci Rep 9, 8664 (. https://doi.org/10.1038/s41598-019-45041-1

Pfafenrot, C., Schneider, T., Müller, C., Hung, L. H., Schreiner, S., Ziebuhr, J., and Bindereif, A. (2021) Inhibition of SARS-CoV-2 coronavirus proliferation by designer antisense-circRNAs. Nucleic Acids Research, 49(21), 12502-12516.

Sarkar, A., and Roy-Barman, S. (2021) Spray-Induced Silencing of Pathogenicity Gene MoDES1 viaExogenous Double-Stranded RNA Can Confer Partial Resistance Against Fungal Blast in Rice. Front Plant Sci. 12:733129. doi: 10.3389/fpls.2021.733129.

Schweizer P, Pokorny J, Abderhalden O, Dudler R (1999) A transient assay system for the functional assessment of defense-related genes in wheat. Mol Plant Microbe Interact 12: 647–654.

Šečić, E. and Kogel, K.H. (2021) Requirements for fungal uptake of dsRNA and gene silencing in RNAi-based crop protection strategies. Current Opinion in Biotechnology, Volume 70, 136-142,ISSN 0958-1669.

Shahid, S., Kim G., Johnson N.R., Wafula E., Wang F., Coruh C., Bernal-Galeano V., Phifer T., dePamphilis C.W., Westwood J.H., et al. (2018) MicroRNAs from the parasitic plant Cuscuta campestris target host messenger RNAs. Nature.;553:82–85. doi: 10.1038/nature25027.

Taning, C.N.T., Arpaia, S., Christiaens, O., Dietz-Pfeilstetter, A., Jones, H., Mezzetti, B., et al. (2019) RNA-based biocontrol compounds: current status and perspectives to reach the market. Pest Manag Sci 76:841-845.

Van Dijk, M, Morley, T, Rau, ML, Saghai, Y (2021) A meta-analysis of projected global food demand and population at risk of hunger for the period 2010–2050. Nature Food 2(7): 494-501.

van Schie, CC, and Takken, FL. (2014) Susceptibility genes 101: how to be a good host. Annu Rev Phytopathol.;52:551-81. doi: 10.1146/annurev-phyto-102313-045854.

Walker, P.L., Ziegler, D.J., Giesbrecht, S. et al., (2023) Control of white mold (Sclerotinia sclerotiorum) through plant-mediated RNA interference. Sci Rep 13, 6477 (2023). https://doi.org/10.1038/s41598-023-33335-4.

Wang, M, Weiberg, A, Lin, FM, Thomma, BP, Huang, HD, and Jin, H. (2016) Bidirectional cross-kingdom RNAi and fungal uptake of external RNAs confer plant protection. Nat Plants. 2:16151. doi: 10.1038/nplants.2016.151.

Wang, Y., Yang, M., Wei, S. et al., (2017) Identification of circular RNAs and their targets in leaves of Triticum aestivum L. under dehydration stress. Front Plant Sci 7:2024

Waugh, A., Gendron, P., Altman, R., Brown, J.W., Case, D., Gautheret, D., Harvey, S.C., Leontis, N., Westbrook, J., Westhof, E., Zuker, M., Major, F. (2002) RNAML: a standard syntax for exchanging RNA information. RNA 8(6):707-17. doi: 10.1017/s1355838202028017.

Weiberg, A., Wang, M., Lin, F. M., Zhao, H., Zhang, Z., Kaloshian, I., and Jin, H. (2013) Fungal small RNAs suppress plant immunity by hijacking host RNA interference pathways. Science, 342(6154), 118-123.

Werner, B.T., Koch, A., Šečić, E., Engelhardt, J., Jelonek, L., Steinbrenner, J., Kogel, K.H. (2021) *Fusarium graminearum* DICER-like-dependent sRNAs are required for the suppression of host immune genes and full virulence. PLoS One. 16(8):e0252365. doi: 10.1371/journal.pone.0252365.

Winkle, M., El-Daly, S.M., Fabbri, M. et al. (2021) Noncoding RNA therapeutics challenges and potential solutions. Nat Rev Drug Discov 20, 629–651 https://doi.org/10.1038/s41573-021-00219-z.

Wu, F. H., Shen, S. C., Lee, L. Y., Lee, S. H., Chan, M. T., and Lin, C. S. (2009) Tape-Arabidopsis Sandwich-a simpler Arabidopsis protoplast isolation method. Plant methods, 5, 1-10.

Wytinck, N., Manchur, C.L., Li, V.H., Whyard, S., and Belmonte, M.F. (2020) dsRNA uptake in plant pests and pathogens: Insights into RNAi-Based Insect and Fungal Control Technology. Plants (Basel). 9(12):1780. doi: 10.3390/plants9121780.

Yang, Y. et al. (2017) Extensive translation of circular RNAs driven by N 6-methyladenosine. Cell Res. 27:626-641.

Yoo, S.-D., Cho, Y.-H., & Sheen, J. (2007) Arabidopsis mesophyll protoplasts: A versatile cell system for transient gene expression analysis. Nature Protocols, 2(7), 1565–1572. https://doi.org/10.1038/nprot.2007.199.

Zabala-Pardo, D, Gaines T, Lamego FP, Avila LA. (2022) RNAi as a tool for weed management: challenges and opportunities. Adv Weed Sci. 40(Spec1):e020220096.

Zand Karimi, H., Baldrich, P., Rutter, B. D., Borniego, L., Zajt, K. K., Meyers, B. C., and Innes, R.W. (2022) Arabidopsis apoplastic fluid contains sRNA-and circular RNA–protein complexes that are located outside extracellular vesicles. The Plant Cell, 34(5), 1863-1881.

Zhang, P, and Dai, M. (2022) CircRNA: a rising star in plant biology. J Genet Genomics. 49(12):1081-1092. doi: 10.1016/j.jgg.2022.05.004

Zhang, P., Li, S., and Chen, M. (2020) Characterization and function of circular RNAs in plants. Front Mol Biosci 7.

Zhang, H., Liu, S., Li, X., Yao, L., Wu, H., Baluška, F., and Wan, Y. (2021) An antisense circular RNA regulates expression of RuBisCO small subunit genes in Arabidopsis. Frontiers in Plant Science, 12, 665014.

Zhang, Y., Zhang, X. O., Chen, T., Xiang, J. F., Yin, Q. F., Xing, Y. H.,et al., (2013) Circular intronic long noncoding RNAs. Molecular Cell, 51(6), 792-806.

Zhu, Y., Zhu, L., Wang, X. *et al.* (2022) NA-based therapeutics: an overview and prospectus. *Cell Death Dis* **13**, 644. https://doi.org/10.1038/s41419-022-05075-2.

Zuker, M. (2003) Mfold web server for nucleic acid folding and hybridization prediction. *Nucleic acids research*, *31*(13), 3406-3415.

Zuo, J., Wang, Q., Zhu, B. et al., (2016) Deciphering the roles of circRNAs on chilling injury in tomato. Biochem. Biophys. Res. Commun. 479:132-138. https://doi.org/10.1016/j.bbrc.2016.07.032.

Fig. 1A

>ORF_GFP_718_bp

…TTTGGAGAGGACAGGGTACCCATCATACTAGTAGATCTGCGATCTAAGTAAGCTTGGCATTCCGGTACTGTTGGTAAAGCCACC**ATG**GTGAGCAAGGGCGAGGAGCTGTTCACCG
GGGTGGTGCCCATCCTGGTCGAGCTGGACGGCGACGTAAACGGCCACAAGTTCAGCGTGTCCGGCGAGGGCGAGGGCGATGCCACCTACGGCAAGCTGACCCTGAAGTTCATCTGC
ACCACCGGCAAGCTGCCCGTGCCCTGGCCCACCCTCGTGACCACCTTGACCTACGGCGTGCAGTGCTTCGC**CCGCTACCCCGACCACATGAAGCAGCACGA**CTTCTTCAAGTCCGC
CATGCCCGAAGGCTACGTCCAGGAGCGCACCATCTTCTTCAAGGACGACGGCAACTACAAGACCCGCGCCGAGGTGAAGTTCGAGGGCGACACCCTGGTGAACCGCATCGAGCTGA
AGGGCATCGACTTCAAGGAGGACGGCAACATCCTGGGGCACAAGCTGGAGTACAACTACAACAGCCACAAGGTCTATATCACCGCCGACAAGCAGAAGAACGGCATCAAGGTGAAC
TTCAAGACCCGCCACAACATCGAGGACGGCAGCGTGCAGCTCGCCGACCACTACCAGCAGAACACCCCCATCGGCGACGGCCCCGTGCTGCTGCCCGACAACCACTACCTGAGCAC
CCAGTCCGCCCTGAGCAAAGACCCCAACGAGAAGCGCGATCACATGGTCCTGCTGGAGTTCGTGACCGCCGCCGGGATCACTCTCGGCATGGACGAGCTGTACAAG**TAA**CTCGACT
AGAGTCGGGGCGGCCGGGGATCCTCTAGAGTCGACCTGCAGGCATGCCGCTGAAATCACCAGTCTCTC…

Fig. 1B

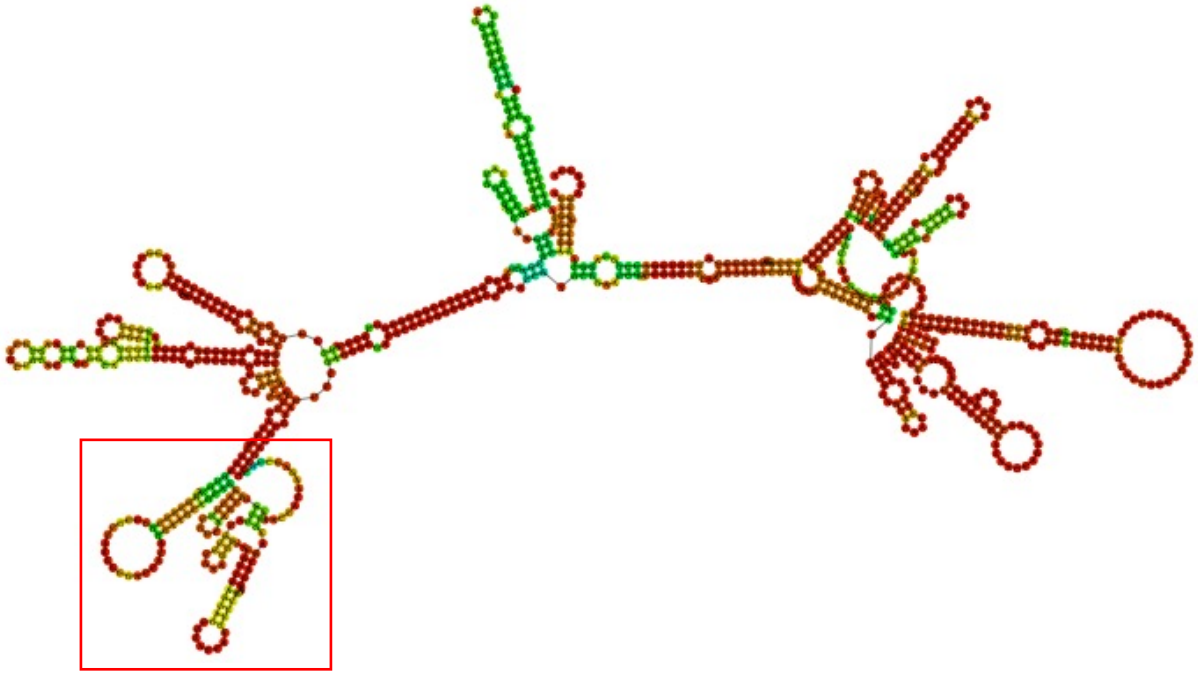

Fig. 1C

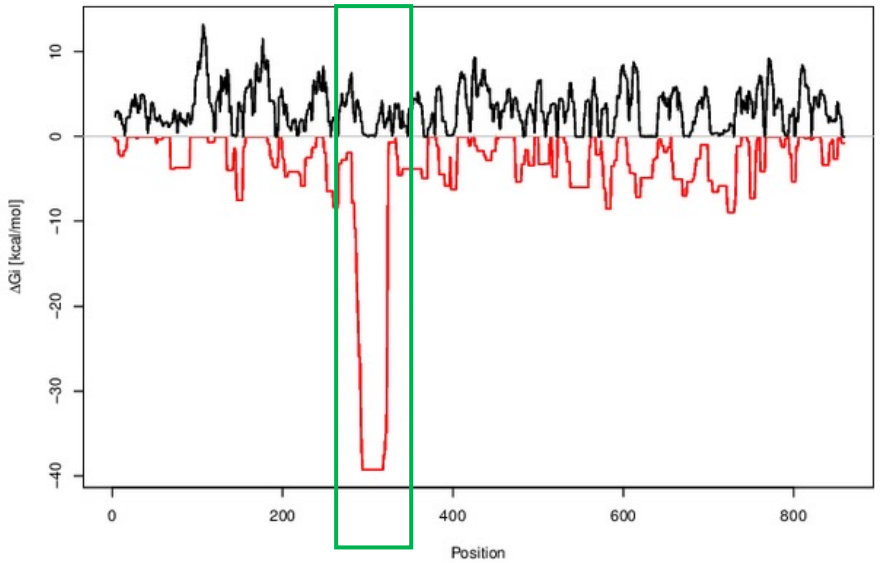

Fig. 1D

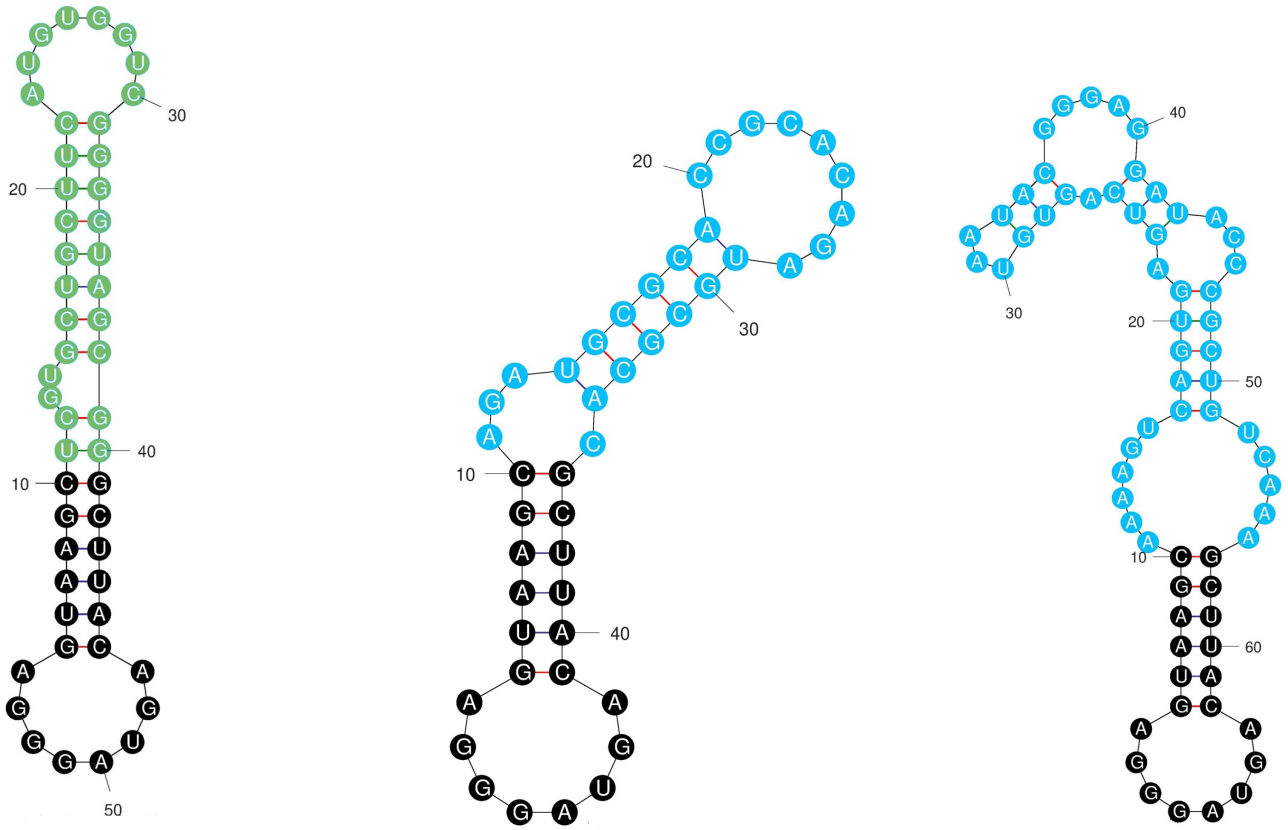

circRNA$_{GFP}$ circRNA$_{CTR1}$ circRNA$_{CTR2}$

Fig. 2A

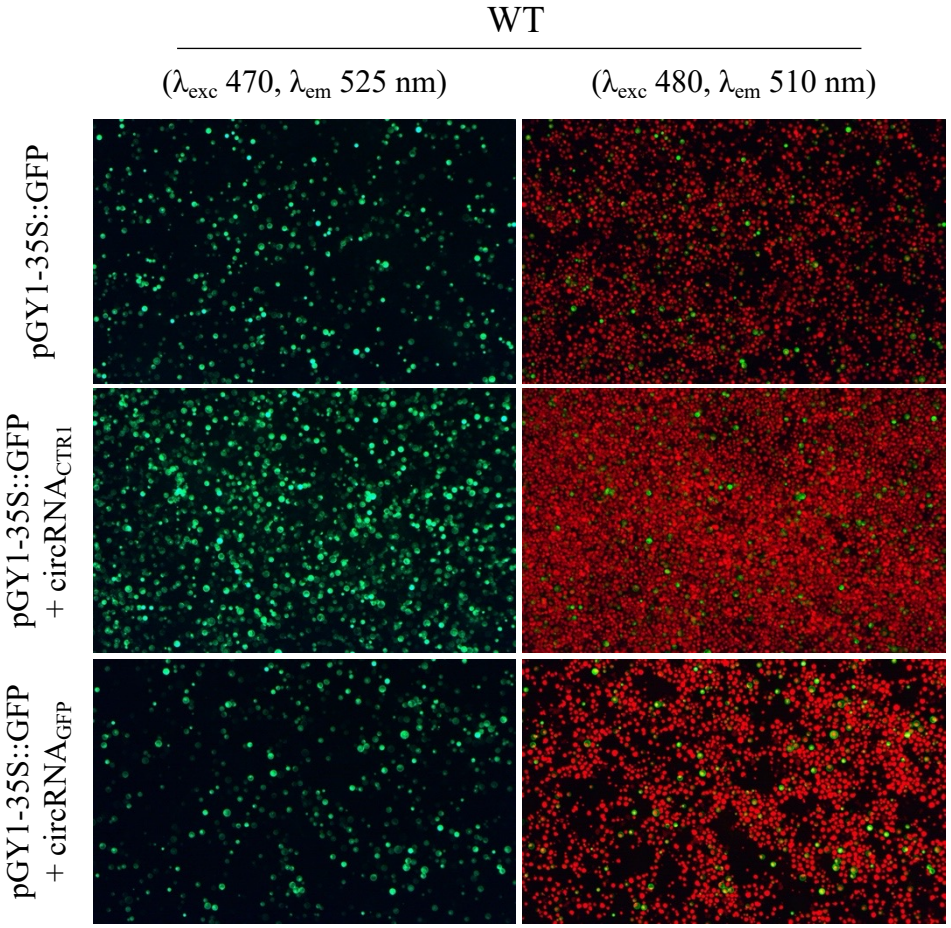
WT
(λ_{exc} 470, λ_{em} 525 nm)
(λ_{exc} 480, λ_{em} 510 nm)
pGY1-35S::GFP
pGY1-35S::GFP + circRNA$_{CTR1}$
pGY1-35S::GFP + circRNA$_{GFP}$

Fig. 2B

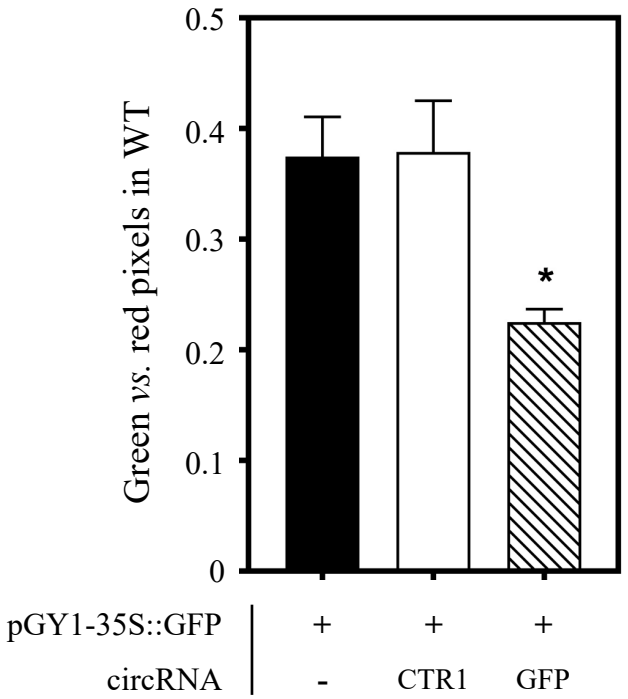
0.5
0.4
0.3
0.2
0.1
0
Green vs. red pixels in WT
*
pGY1-35S::GFP
+
+
+
circRNA
-
CTR1
GFP

Fig. 3

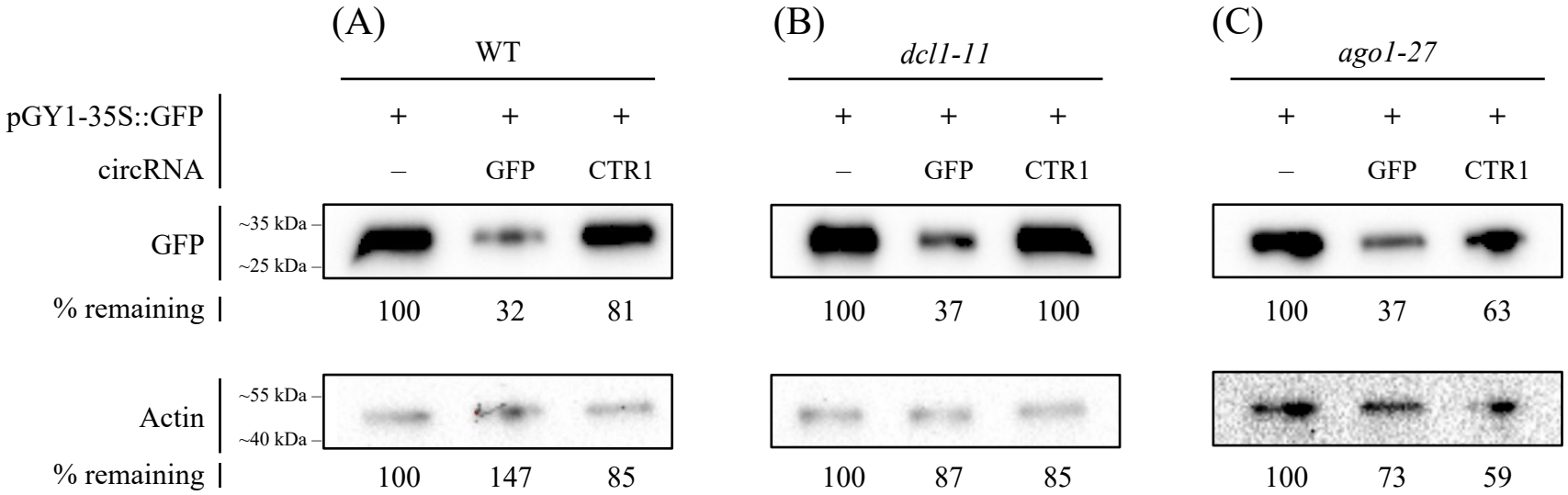

	(A) WT			(B) *dcl1-11*			(C) *ago1-27*		
pGY1-35S::GFP	+	+	+	+	+	+	+	+	+
circRNA	–	GFP	CTR1	–	GFP	CTR1	–	GFP	CTR1
% remaining (GFP)	100	32	81	100	37	100	100	37	63
% remaining (Actin)	100	147	85	100	87	85	100	73	59
GFP/ACTIN	**1**	**0.22**	**0.95**	**1**	**0.43**	**1.17**	**1**	**0.51**	**1.06**

Fig. 4

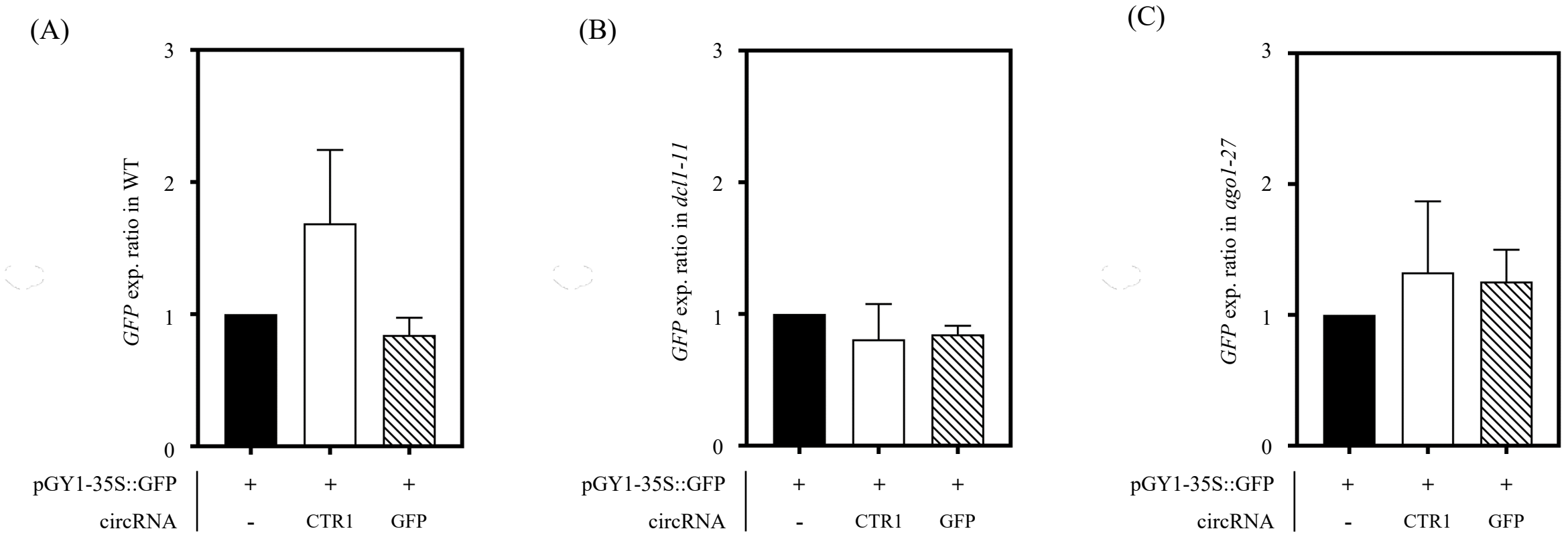
(A)
GFP exp. ratio in WT
3
2
1
0
pGY1-35S::GFP + + +
circRNA - CTR1 GFP
(B)
GFP exp. ratio in dcl1-11
3
2
1
0
pGY1-35S::GFP + + +
circRNA - CTR1 GFP
(C)
GFP exp. ratio in ago1-27
3
2
1
0
pGY1-35S::GFP + + +
circRNA - CTR1 GFP

Fig. 5

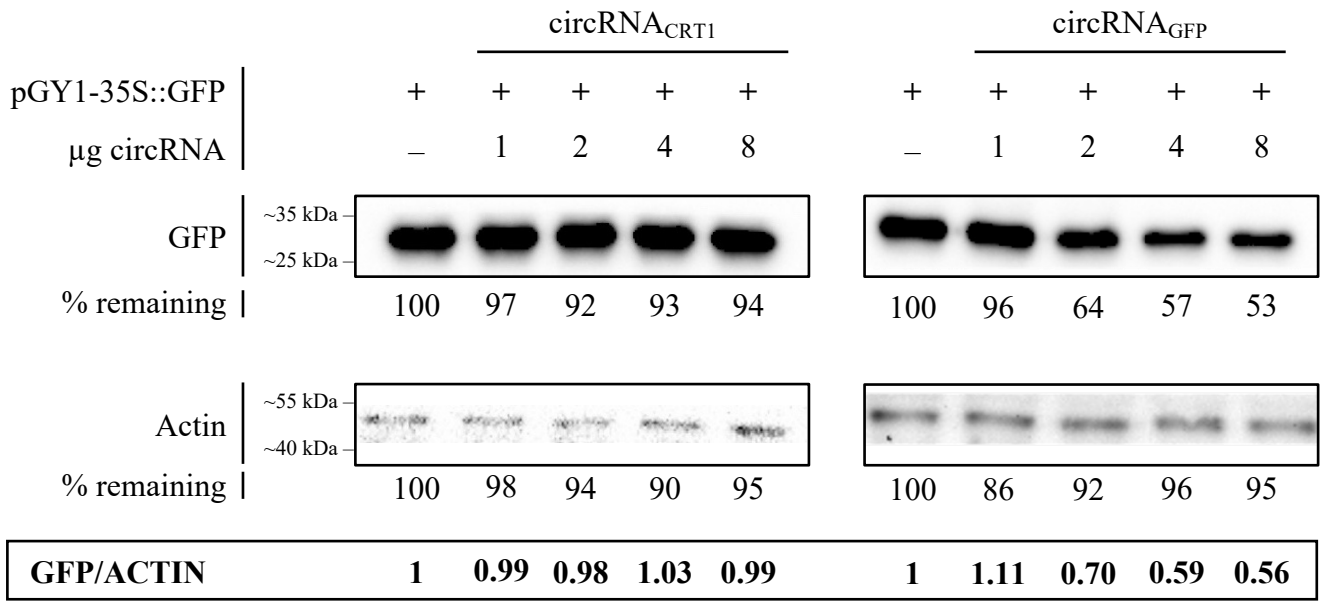
circRNA$_{CRT1}$
circRNA$_{GFP}$
pGY1-35S::GFP
+ + + + + + + + + +
µg circRNA
– 1 2 4 8 – 1 2 4 8
GFP
~35 kDa
~25 kDa
% remaining
100 97 92 93 94 100 96 64 57 53
Actin
~55 kDa
~40 kDa
% remaining
100 98 94 90 95 100 86 92 96 95
GFP/ACTIN
1 0.99 0.98 1.03 0.99 1 1.11 0.70 0.59 0.56

Fig. 6

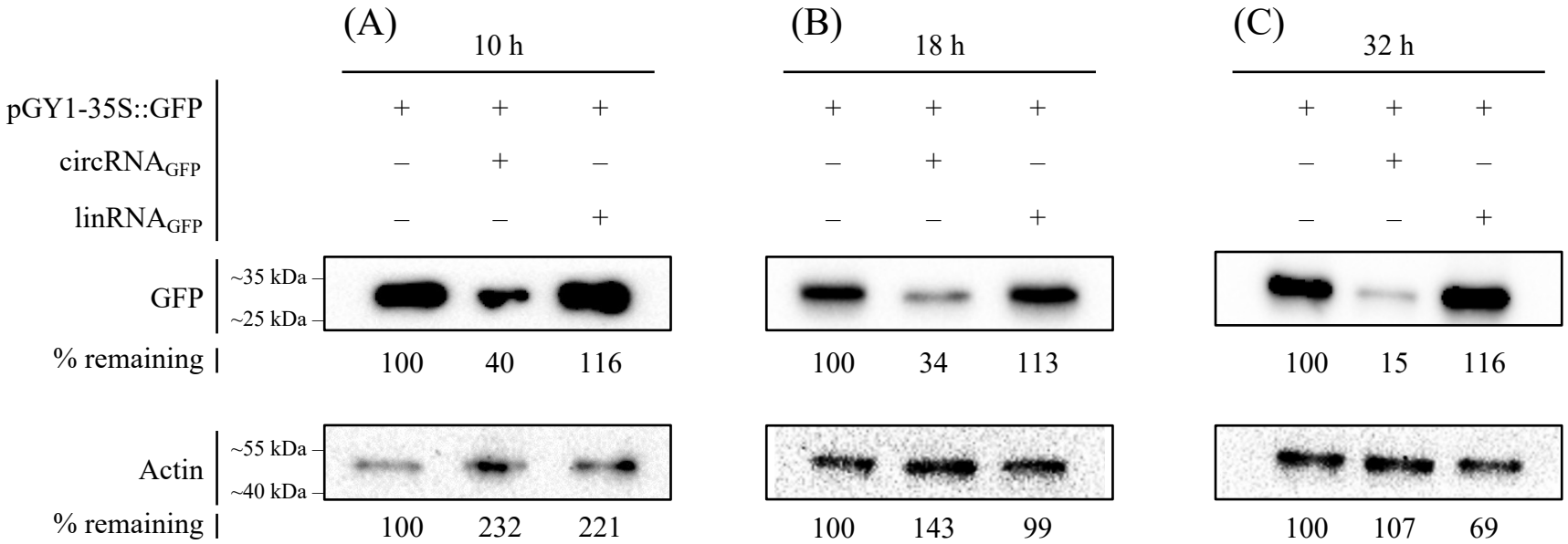

GFP/ACTIN	**1**	**0.17**	**0.52**	**1**	**0.24**	**1.14**	**1**	**0.14**	**1.68**

Fig. 7A

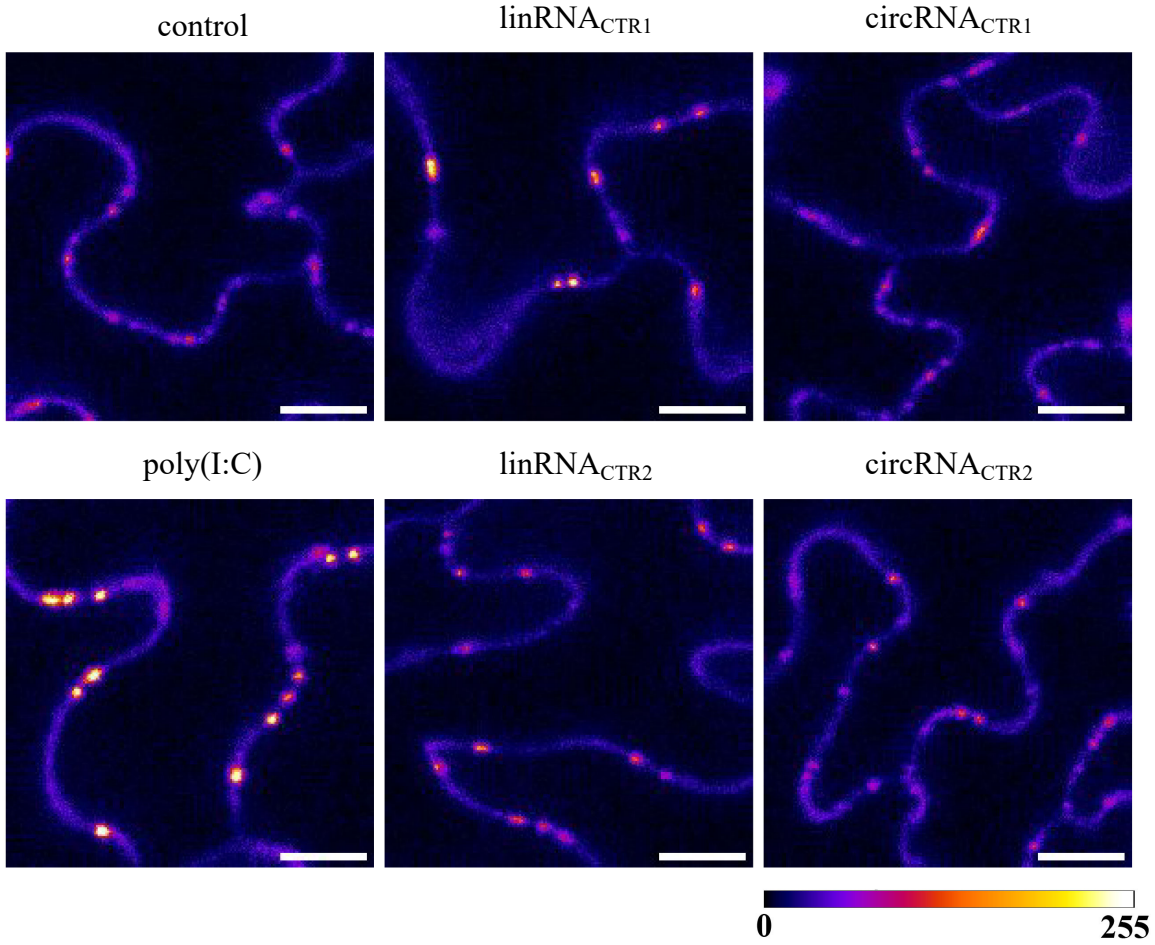
control
linRNA$_{CTR1}$
circRNA$_{CTR1}$
poly(I:C)
linRNA$_{CTR2}$
circRNA$_{CTR2}$
0
255

Fig. 7B

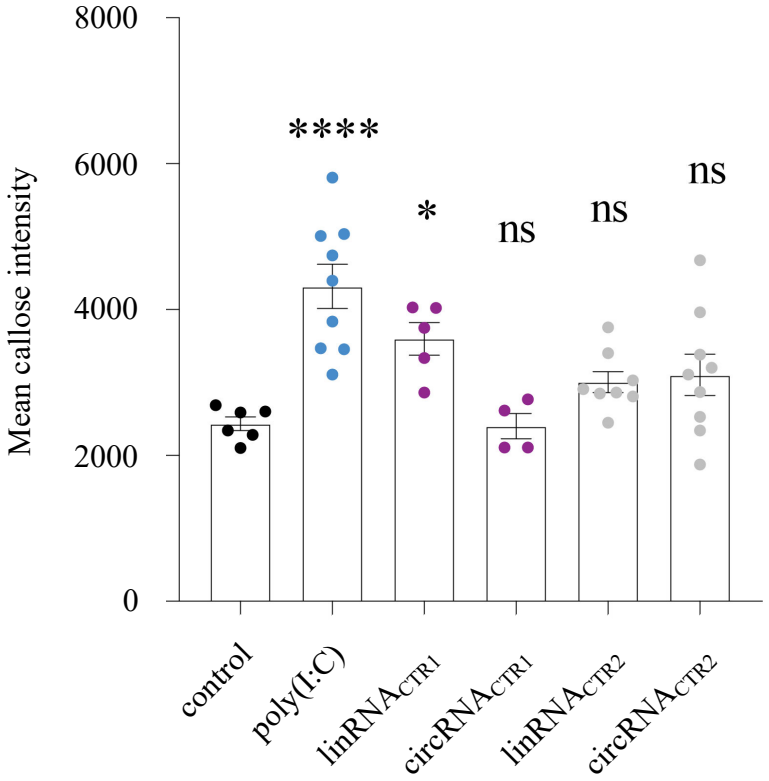
Mean callose intensity
8000
6000
4000
2000
0
****
*
ns
ns
ns
control
poly(I:C)
linRNA$_{CTR1}$
circRNA$_{CTR1}$
linRNA$_{CTR2}$
circRNA$_{CTR2}$